Asian Journal of Chemistry; Vol. 28, No. 7 (2016), 1413-1416

ASIAN JOURNAL OF CHEMISTRY

http://dx.doi.org/10.14233/ajchem.2016.19638

Synthesis, Characterization of Si/Fe_2O_3 Nanoparticles and their Antibacterial Activity against *Staphylococcus aureus* and *Escherichia coli*

MUHAMMAD ARSHAD[1], MUHAMMAD AKHYAR FARRUKH[1,*], RAJA ADIL SARFRAZ[2] and AYESHA IMTIAZ[1]

[1]Nano-Chemistry Lab., Government College University, Lahore-5400, Pakistan
[2]Department of Chemistry, University of Agriculture, Faisalabad-38040, Pakistan

*Corresponding author: E-mail: akhyar100@gmail.com

Received: 26 September 2015; *Accepted*: 13 February 2016; *Published online*: 31 March 2016; AJC-17822

Silicon doped iron oxide (Si/Fe_2O_3) nanoparticles were successfully synthesized by co-precipitation method at 60 °C with 2-propanol as solvent. The particle size of Si/Fe_2O_3 nanoparticles measured with transmission electron microscope and dynamic light scattering techniques are nearly same (36.65 nm). The properties of Si/Fe_2O_3 nanoparticles are different than core shell SiO_2/Fe_2O_3 nanoparticles as they show aggregation and antibacterial properties. Its antibacterial effect was studied against *Staphylococcus aureus* and *Escherichia coli* which showed the significant results. The other structural characteristics of the Si/Fe_2O_3 nanoparticles were analyzed by scanning electron microscope, X-ray diffraction, thermal gravimetric analysis and Fourier transform infrared spectroscopy.

Keywords: Synthesis, Characterization, Antibacterial activity, *Staphylococcus aureus*, *Escherichia coli*.

INTRODUCTION

In recent years, nanoscale magnetic nanoparticles mostly used in drug delivery system, enzyme immobilization, protein separation, magnetic resonance imaging for cancer diagnosis. Now a day's bio-fishing is an interesting tool in biomedical applications [1-6]. Silica-coated magnetic nanoparticles treated with amino-silane as coupling agent, which have $–NH_2$ group that can be transferred to aldehyde group, that easily connect to proteins, enzymes and drugs [7-12].

Successful incorporation of metals in metal oxide nanoparticles have been made by using hydrothermal, ultrasonication, sol gel and co-precipitation methods [13,14]. Silica coated magnetic nanoparticles were synthesized by sol-gel [15,16] and co-precipitation method [17,18]. The mechanism of this reaction is that Fe^{2+} ions react with –OH group radicals in aqueous media, thus magnetic nanoparticles are formed. Silica-coated Fe_2O_3 nanoparticles prepared by co-precipitation method have large number of –OH groups on the surface of precipitates. The most important factor for the synthesis of silica-doped magnetic nanoparticles are the particle size, their distribution, super magnetic properties, hydrophilicity and hydrophobic properties [19,20]. Iron oxide nanoparticles are known for their biocompatibility and use in MRI technique. When these nanoparticles are coated with silica, their super magnetic properties are suppressed by sheltering magnetic dipole interactions and particles do not aggregate [21,22].

The present work reports the synthesis of Si/Fe_2O_3 nanoparticles by co-precipitation method at 60 °C by using 2-propanol as solvent and their antibacterial activity was observed against Gram-positive and Gram-negative bacteria. Hence, we make use of this work to inhibit growth of *Staphylococcus aureus* and *Escherichia coli* using selective nutrient broth. Bacterial strains which selected in this work were highly contagious, that is why we can easily evaluate the antibacterial potential of Si/Fe_2O_3 nanoparticles.

EXPERIMENTAL

All the chemicals used were of analytical grade including commercial iron oxide, concentrated nitric acid (Merck), ethyl alcohol (Biom), tetraethyl orthosilicate (TEOS) (Aldrich 98 %), tartaric acid (Panreac). All the chemicals were used in purchased form without any further purification.

Characterization techniques: FTIR (Shimadzu) was used for structural characterization of synthesized Si/Fe_2O_3 nanoparticles. Crystal structure and crystallite size was determined by X-ray diffraction (Philips X' Pert), scanning electron microscopy (JEOL 7600) and transmission electron microscopy (Philips CM12) was done to study morphology and determination of particles size. Thermogravimetric analysis of uncalcined nanoparticles was carried out by TGA/SDT G600 V8.3 Build 101. Furnace (VULCAN D-550) was used for calcination of nanoparticles.BT-90 Nano Particle size analyzer.

Preparation of Si/Fe_2O_3 nanoparticles: Tetraethyl orthosilicate (4.75 g) and 0.15g of tartaric acid were added in 10 mL of 2-propanol and stirred for 20 min to make the homogenous mixture. Then 20 mL of NH_3:H_2O mixture was added in the mixture (pH = 9). 0.5 g of Fe_2O_3 was added in 10 mL of 2-propanol in a separate beaker and heated for 3 h by continuous stirring at 60 °C on hot plate with reflux condenser. This mixture of Fe_2O_3 was poured in the above prepared mixture while stirring. 2 mL of ammonia solution was added in the reaction mixture drop by drop and pH was adjusted at 8.5. The reaction mixture was stirred for another 3 h at 60 °C and then centrifuged at 3000 rpm for 40 min. The precipitates were separated and washed several times with deionized water and ethanol and dried overnight at 70 °C. Finally the product was calcined at 500 °C for 3 h.

Antibacterial activity: Antibacterial activity of Si/Fe_2O_3 nanoparticles was determined by using disc diffusion method and measuring zone of inhibition [23]. Two bacterial strains *Staphylococcus aureus* (Gram-positive) and *Escherichia coli* (Gram-negative) were used for antibacterial activity, which were obtained from Department of Microbiology, University of Agriculture, Faisalabad. Nutrient agar (Oxoid, UK) was prepared, medium heated mixed and then autoclaved. Before transferring this medium in sterilized petri plates, 100 mL inoculum was added in medium while it was liquid and quite cool. Mixed and then pour into Petri plates. After this, 6 mm wicks paper discs were laid flat on growth medium and 100 µL of Si/Fe_2O_3 nanoparticles was put on each disc. The petri plates were then incubated at 37 °C for 24 h, for the growth of bacteria. The Si/Fe_2O_3 nanoparticles having antibacterial activity, inhibited the bacterial growth and clear zone of inhibition was formed. The zones of inhibition were measured in millimetres using zone reader.

RESULTS AND DISCUSSION

Thermogravimetric analysis: TGA curve (Fig. 1) showed the major weight loss into three distinct steps. In the first step, 1.25 % weight loss occurred from 25 to 50 °C which may be attributed to loss or volatilization of small malleable, such as H_2O and absorbed NH_3:H_2O. In the second step, 11.25 % weight loss is from 50 to 260 °C which is much closer to the theoretical weight loss (11.27 %) of water from $Si(OH)_4$ during the formation of Si/Fe_2O_3 nanoparticles. From 260 to 500 °C there is slight weight loss of 2.5 % which can be attributed to the free water molecules intricate in the crystal structure of nanoparticles.

FTIR characterization: Fig. 2 shows a wide peak present in range 3400 to 3000 cm^{-1} which represents the presence of –OH on the surface of nanopartilces. A sharp peak present at 1129 cm^{-1} can be attributed to the Si–O–Si bond asymmeteric stretching vibrations and a small peak at 950 cm^{-1} represents Si–O bond stretching vibrations. Asymmetric stretching vibrations of Fe–O bond can be observed at 804 and 549 cm^{-1} while O–Si–O bond bending vibrations are observed at 474 cm^{-1}. Other small peaks present at 2337, 1869 and 1629 cm^{-1} are due to remains of organic solvent used during the synthesis of nanoparticles [24].

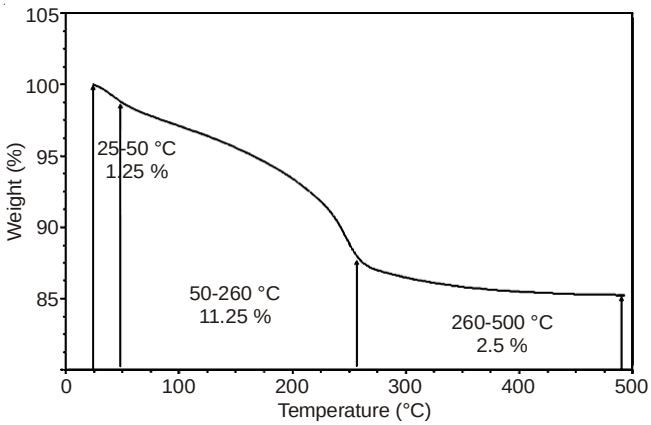

Fig. 1. TGA analysis of Si/Fe_2O_3 nanoparticles

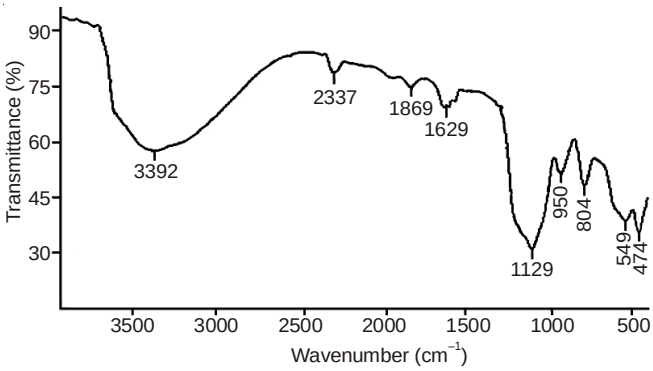

Fig. 2. FTIR spectra of Si/Fe_2O_3 nanoparticles

XRD characterization: In Fig. 3, the peaks present at 2θ = 24.13° (012), 35.6° (110), 49.4° (024), 54.04° (116), 62.4° (214) and 63.49° (300) represent the formation of Fe_2O_3 nanoparticles with rhombohedral crystal structure and are well indexed with ICDD data base (PDF# 00-024-0072). The sharp peak present at 2θ = 33.17° (201) and a small peak at 57.62° (331) represents the doped Si on Fe_2O_3 nanoparticles (PDF# 00-40-0932). These results revealed the successful doping of Si on Fe_2O_3 nanoparticles. XRD data were used to estimate mean size of Si/Fe_2O_3 nanoparticles by using the Scherrer's equation explained:

$$D = \frac{K\lambda}{B\cos\theta}$$

Average crystallite size for Si doped Fe_2O_3 nanoparticles was 8.38 nm.

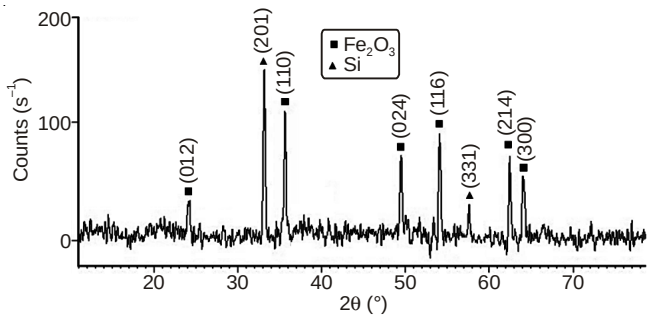

Fig. 3. XRD spectra of Si-doped Fe_2O_3 nanoparticles

SEM analysis: Fig. 4 show SEM micrograph of Si/Fe_2O_3 nanoparticles synthesized by co-precipitation method and calcined at 500 °C. It shows the spherical Si scattered on the rough surface of Fe_2O_3 nanoparticles.

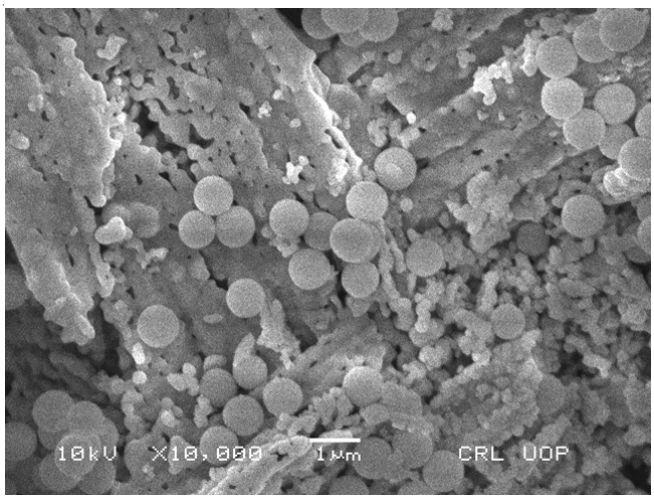

Fig. 4. SEM analysis of Si/Fe_2O_3nanoparticles

TEM analysis: Fig. 5 shows a TEM micrograph of Si-doped Fe_2O_3 nanoparticles prepared and calcined at 500 °C for 3 h. The Si/Fe_2O_3 nanoparticles seems to aggregate into large clusters. The reason of large clusters is strong dipole-dipole attractions and magnetic force between the nanoparticles as silica did not encapsulate the Fe_2O_3 nanoparticles. The particles size of Si/Fe_2O_3 nanoparticles is 35-37 nm.

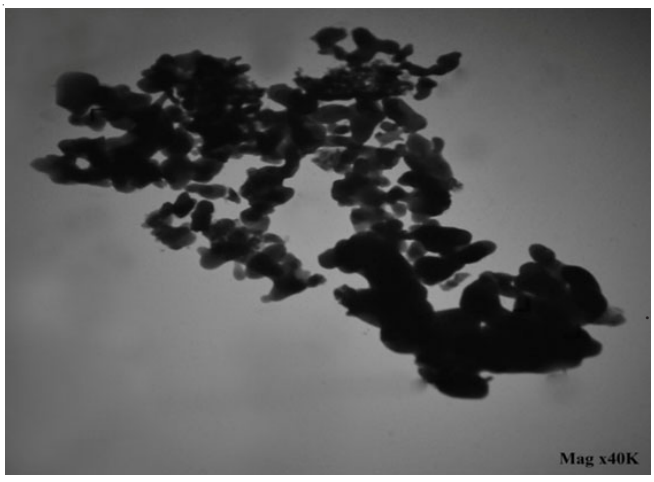

Fig. 5. TEM image of Si-doped Fe_2O_3 nanoparticles

Dynamic light scattering analysis: 0.1 M solution of Si/Fe_2O_3 nanoparticles was used to determine the hydrodynamic diameter of the synthesized nanoparticles. Hydrodynamic diameter of the nanoparticles usually larger than their size due to presence of stabilizer at their surface. Fig. 6 shows the number distribution of Si/Fe_2O_3 nanoparticles synthesized by co-precipitation method. The highest peak in the Fig. 6 showed the 36.65 nm size of Si/Fe_2O_3 nanoparticle which is close size measured by TEM analysis.

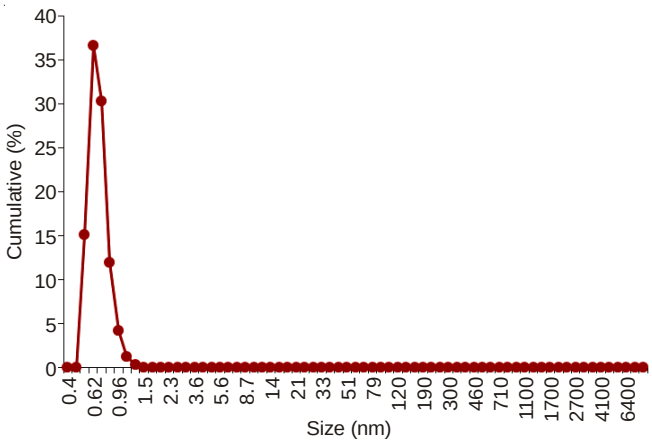

Fig. 6. Dynamic light scattering of Si-doped Fe_2O_3 nanoparticles

Antibacterial activity: Antibacterial activity of Si/Fe_2O_3 was investigated by using disc diffusion method on the basis of inhibition zone size (mm). The antibacterial activity showed significant reduction in bacterial growth in terms of zone inhibition around the disc. The Si/Fe_2O_3 showed approachable inhibition of the growth *Staphylococcus aureus* 13.5 mm while standard used rifampicin showed significant inhibition 24 mm as shown in Fig. 7. The Si/Fe_2O_3 nanoparticles showed significant inhibition 5 mm against *Escherichia coli* but it is much less than the standard (rifampicin) as showed 27 mm.

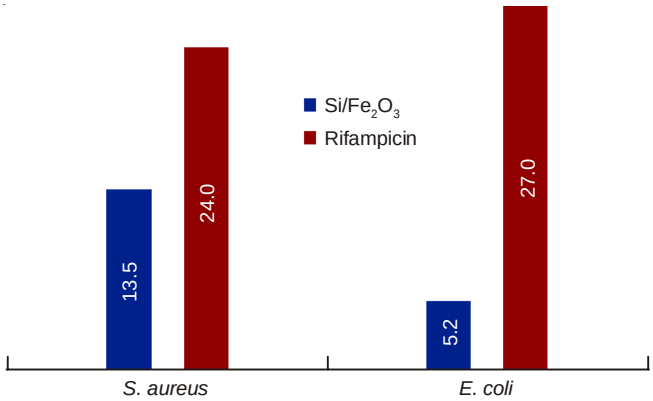

Fig. 7. Antibacterial activity of Si/Fe_2O_3 nanoparticles

Conclusion

Synthesis of Si/Fe_2O_3 nanoparticles was successfully carried out by using co-precipitation method at 60 °C. Different characterization such as transmission electron microscope, scanning electron microscope, X-ray diffraction, thermal gravimetric analysis-differential scanning calorimetry, dynamic light scattering analysis and Fourier transform infrared spectroscopy was performed. These detailed fundamental characterizations revealed that the synthesized Si/Fe_2O_3 nanoparticles are crystalline and spherical in their structure and have diameter range from 30-37 nm. Furthermore these nanoparticles were also investigated for their practical importance such as antibacterial activity. Two microbes *Staphylococcus aureus* and *Escherichia coli* were used for this activity. The Si/Fe_2O_3 nanoparticles showed the significant results against both microbes.

REFERENCES

1. A. Elaissari and V. Bourrel, *J. Magn. Magn. Mater.*, **225**, 151 (2001).
2. M. Koneracka, P. Kopcansky, M. Antalik, M. Timko, C. Ramchand, D. Lobo, R. Mehta and R. Upadhyay, *J. Magn. Magn. Mater.*, **201**, 427 (1999).
3. H. Gries, W. Mutzel, C. Zurth and H.J. Weinmanm, Magnetic Particles for Diagnostic Purposes, US Patent 5746999 (1998).
4. D.K. Kim, Y. Zhang, W. Voit, K.V. Rao and M. Muhammed, *J. Magn. Magn. Mater.*, **225**, 30 (2001).
5. Y.H. Choa, J.K. Yang, W.J. Yang and K.H. Auh, *J. Magn. Magn. Mater.*, **266**, 20 (2003).
6. E.T. Fung, V. Thulasiraman, S.R. Weinberger and E.A. Dalmasso, *Curr. Opin. Biotechnol.*, **12**, 65 (2001).
7. A.K. Singh, A.W. Flounders, J.V. Volponi, C.S. Ashley, K. Wally and J.S. Schoeniger, *Biosens. Bioelectron.*, **14**, 703 (1999).
8. A.S. Piers and C.H. Rochester, *J. Colloid Interf. Sci.*, **174**, 97 (1995).
9. H. Okabayashi, I. Shimizu, E. Nishio and C.J.O. Connor, *Colloid Polym. Sci.*, **275**, 744 (1997).
10. K.C. Vrancken, L. De Coster, P. Van Der Voort, P.J. Grobet and E.F. Vansant, *J. Colloid Interf. Sci.*, **170**, 71 (1995).
11. S.T. Lim, M.S. Cho, H.J. Choi and M.S. Jhon, *J. Ind. Eng. Chem.*, **9**, 336 (2003).
12. M.S. Cho, S.T. Lim, I.B. Jang, H.J. Choi and M.S. Jhon, *IEEE Trans. Magn.*, **40**, 3036 (2004).
13. I. Muneer, M.A. Farrukh, S. Javaid, M. Shahid and M. Khaleeq-ur-Rahman, *Superlattices Microstruct.*, **77**, 256(2015).
14. S. Javaid, M.A. Farrukh, I. Muneer, M. Shahid, M. Khaleeq-ur-Rahman and A.A. Umar, *Superlattices Microstruct.*, **82**, 234 (2015).
15. K. Kim and H. Kim, *J. Sol-Gel Sci. Technol.*, **25**, 183 (2002).
16. O.K. Park, Y.S. Kang and B.G. Jo, *J. Ind. Eng. Chem.*, **10**, 733 (2004).
17. S.A. Chulovskaya, K.N. Zheleznov and O.V. Zemtsova, *Colloid J.*, **65**, 786 (2003).
18. Y.S. Kang, S. Risbud, J.F. Rabolt and P. Stroeve, *Chem. Mater.*, **8**, 2209 (1996).
19. S. Tao, X. Liu, X. Chu and Y. Shen, *Sens. Actuators B*, **61**, 33 (1999).
20. X. Liu, Z. Ma, J. Xing and H. Liu, *J. Magn. Magn. Mater.*, **270**, 1 (2004).
21. W. Stöber, A. Fink and E. Bohn, *J. Colloid Interf. Sci.*, **26**, 62 (1968).
22. M. Ohmori and E. Matijeviæ, *J. Colloid Interf. Sci.*, **150**, 594 (1992).
23. T. Naseem and M.A. Farrukh, *J. Chem.*, **2015**, 1 (2015).
24. E. Doelsch, W.E.E. Stone, S. Petit, A. Masion, J. Rose, J.-Y. Bottero and D. Nahon, *Langmuir*, **17**, 1399 (2001).